# The Safety Factor Approach in the Analysis of Reentrant Patterns of Activation in the Ischemic Virtual Heart

L Romero, B Trenor, JM Ferrero (Jr), J Sáiz,
G Moltó, JM Alonso

Universidad Politécnica de Valencia, Valencia, Spain

## Abstract

*Traditionally, VF has been directly related to dispersion of refractoriness. However, further theoretical studies relating refractoriness and reentry generation would be helpful to understand their implication. Recently, the safety factor for conduction (SF) has been proposed as a useful parameter to analyze propagation of action potential (AP) and conduction block.*

*In this work, the relative role of refractoriness and the source-sink relationship in conduction block leading to reentry during regional ischemia has been analyzed.*

*Our results show that a) premature stimuli applied at CIs comprised between 170 ms and 204 ms lead to reentry, b) the distribution of SF during reentry is very similar for all the conducted simulations and c) in one third of the re-entries the premature stimulus was blocked at sites where the excitability of the cells was completely recovered.*

## 1. Introduction

Ventricular tachycardia (VT) and ventricular fibrillation (VF) are potentially lethal arrhythmias frequently caused by reentrant electrical activity in heart ventricles [1]. So, there always has been a great interest in the study of initiation and maintenance of the re-entrant activity. It is well known that heterogeneity of electrophysiological properties in the ventricular tissue, such as conduction velocity, membrane excitability and refractoriness, is crucial for the genesis of re-entrant arrhythmias [2, 3, 4]. In particular, much attention has been paid to the dispersion of refractoriness. Traditionally, this parameter has been considered as proarrhythmic [Allessie et al. 1967 referenced by 2 y 4], although some authors disagree with this hypothesis [Naimi et al. 1977 referenced by 2, 5].

It is well known that VT and VF usually arise during myocardial ischemia [1], when important electrophysiological cellular changes take place. Indeed, acidosis, hyperkalemia and hypoxia observed during ischemic episodes affect action potential (AP) morphology and propagation.

In the last years, a quantitative parameter related to the source-sink relationship of propagation has been defined. This parameter has been called safety factor (SF) and has given interesting insights to AP propagation process and block [6, 7, 8, 9]. Furthermore, its recent extension to 2D [9] enables its use in bidimensional tissues.

In this paper, we have studied the vulnerability to reentry under ischemic conditions and then, the source-sink relationship has been quantified by means of the SF in order to reveal the relative role of refractoriness in reentry generation.

## 2. Methods

Cellular electrical activity was simulated using a modified version of the Luo-Rudy dynamic AP model (LRd00) [10].

Acute ischemia was reproduced by means of its three main components. For this purpose, the affected parameters were set according to those values experimentally observed at different instants after the onset of ischemia, as shown in Figure 1. Firstly, hypoxia was considered by partially activating the ATP-sensitive $K^+$ current ($I_{K(ATP)}$), formulated by Ferrero Jr. et al. [11]. For this purpose, intracellular concentration of ATP and ADP were increased from 6.8 mmol/L and 15 mol/L in the normal zone (NZ) up to 4.6 mmol/L and 78 mol/L in the central zone (CZ) respectively [12, 11]. Secondly, hyperkalemia was simulated by elevating extracellular $K^+$ concentration ($[K^+]_0$). In particular, $[K^+]_o$ was set to a value of 5.4 mmol/L in the NZ increasing up to 12.5 mmol/L in the CZ [12, 3]. Finally, acidosis was taken into account by its effect on the $Na^+$ and $Ca^{2+}$ current [7,8]. Hence, the fast inward $Na^+$ current ($I_{Na}$) and the $Ca^{2+}$ current through the L-type channels ($I_{Ca(L)}$) were affected by a factor $f_{pH}$ of 0.875 in the CZ [13, 14].

Figure 1b depicts the cardiac tissue of 5.5 cm x 5.5 cm, which includes a NZ and a circular central CZ of 2 cm in diameter surrounded by a 1 cm thick ring-shaped ischemic border zone (BZ).

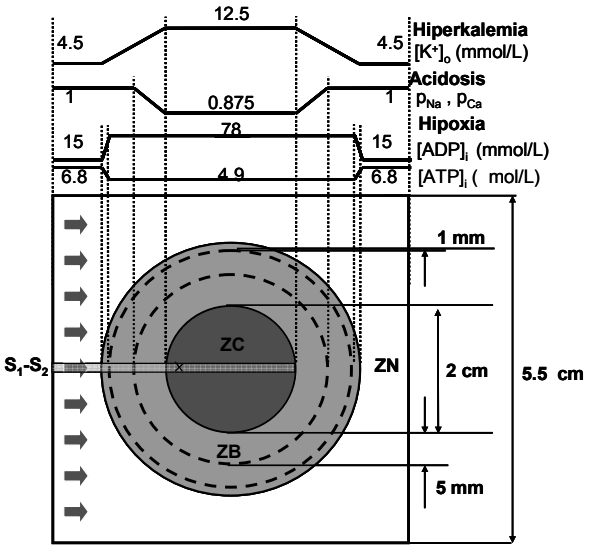


Figure 1. 5.5 cm x 5.5 cm regional ischemic tissue composed by the normal zone (NZ), the circular central ischemic zone (CZ) and the ring-shaped border zone (BZ). The electrophysiological properties vary linearly along the border zone reaching the ischemic values in the CZ. The rectangle and the cross represent the considered fibre for the PR obtention and the site where it is measured.

In the ischemic BZ, all parameters return to their normal values along linear spatial gradients (see Fig. 1, panel (b)), following experimental observations reported by Coronel [15]. Hyperkalemia experienced a linear increase along 1 cm of tissue, fraction of activated K(ATP) channels ($f_{ATP}$) increased along 0.1 cm of tissue and the decrease of sodium and calcium channels activation took place along the inner 0.5 cm of the BZ.

The stimulation protocol consisted of two rectangular current pulses (S1–S2), of 2 ms in duration and an amplitude of twice the diastolic threshold. Both pulses were delivered at the left edge of the tissue, longitudinal to fibre orientation.

Probability of reentry was measured by means of the vulnerable window (VW). This parameter was defined as the interval of CIs for S2 delivery that led to reentry.

In this work, the effective refractory period (ERP) of the cell of the central fibre where propagation blocks was obtained as the ERP of cell 222 of a unidimensional fibre. This fibre mimics the behaviour of the first 375 cells of the central fibre of the simulated tissue (Figure 1). In this case, an S1-S2 protocol of 2 ms in duration and with an amplitude of twice the diastolic threshold was applied at different CIs in cell 222. The ERP was considered as the minimum CI developing AP.

To assess the role of refractoriness leading to UDB, a novel method was applied. Firstly, the SF analysis was required in order to identify the exact location of the line block. This zone was defined as the area where the SF drops below unity. Secondly, the instant when the extrestimulus reaches the cell of block was compared to the end of its refractoriness. If the activation time (AT) of the extraestimulus was prior to the recovery of the cell, propagation block was due to refractoriness. The AT was considered as the instant when the derivative of the membrane potential reached its maximum and the end of refractoriness was calculated as the addition of the ERP to the AT of the basic stimulus. In order to simplify this method, only the central fibre of the tissue was tested, as it is the most likely cell to remain unrecovered.

## 3. Results

Conducted simulation resulted in figure-of-eight reentry whenever CI of S1-S2 protocol was comprised between 170 and 204 ms, which means that the width of the VW was 35 ms. Besides, the reentrant episodes were very stable, completing three cycles at least. Figure 2 displays colour-coded snapshots of the membrane potentials for the first two cycles of the re-entrant activity provoked by an extraestimulus of 194 ms of CI.

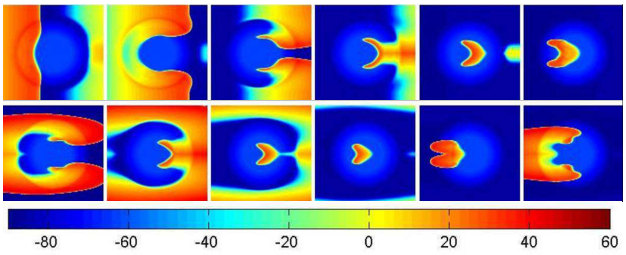


Figure 2. Snapshots of the membrane potential taken during the two first cycles of a reentry (CI=194 ms). Red colour represents depolarization and blue colour reproduces resting potential. The first snapshot shows the instant 65 after extraestimulation and continuous picture are spaced in 60 ms.

Figure 3 illustrates the quantification of the source-sink relationship throughout the ischemic tissue for the first cycle of the reentry observed at CI of 193 ms. Although this phenomenon involves multiple activation of every cell, panel 3 A only represents (by means of contour lines) the SF of the first activation of every cell produced by the extraestimulus. However, panel 3 B, which displays the SF registered for the central fibre, consists of two curves, the thin curve describes the source-sink relationship for the anterograde propagation, whereas the thick one shows the SF for the retrograde sense.

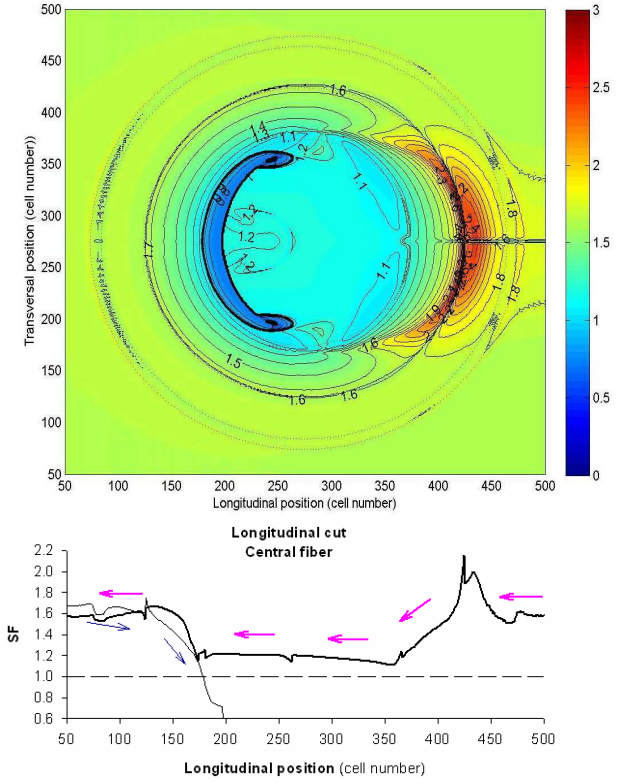


Figura 3. SF in a regional ischemic tissue for a reentry (CI of 193 m). A: Colour-coded representation and contour lines (0.1 increment) of the SF during the first cycle of a reentrant episode. Dotted lines delimitate the different BZs. B: SF of the central fiber for anterograde (thin line) and retrograde propagation (thick line). Arrows indicate the sense of the propagation, anterograde (blue thin line) and retrograde (pink thick line).

As can be seen in Figure 3, the impulse started to propagate with a uniform SF of 1.67 approximately, which is in close agreement with other studies [9]. When the impulse reaches the BZ, the source-sink relationship monotonally begins incrementing its value up to 1.75. Then it decreases and drops below unity at the proximal CZ when the propagation fails. Not only the elevation of the SF is consistent with other simulation studies [7, 8, 9], but also the coincidence of the drop of the SF below unity with propagation block [6, 7, 8, 9]. However, S2 is able to propagate through the NZ and the BZ, so the wavefront splits in two and the SF maintains its value close to 1.7 until reaching the distal zone (see third snapshot of Figure 2). Then, both waves collide and the SF rises its value reaching the maximum (2.7) in the BZ. This increase is also explained by the transverse propagation of S2. However, the source sink relationship is not as safe as the one recorded for transversal propagation under normal conditions (2.9) [8]. Two factors might explain this phenomenon. On the one hand, the wavefront is convex, and on the other hand, acute ischemia reduces excitability [9]. While the extraestimulus propagates through the inner distal BZ, the safety decreases significantly and reaches at the CZ with a value close to unity. However, the SF does not drop below unity and remains quite stable at 1.2 in the CZ, which allows the propagation in the anterograde sense. Hence, S2 is conduced through the CZ and arrives at the proximal BZ and the NZ completing the reentrant pathway.

It is to be noticed that for all the observed reentries the SF patterns are very similar and the arch of block is placed at the proximal area of the CZ.

Once the analysis of the SF during reentrant episodes has been carried out, the implication of the RP in the genesis of the UDB leading to reentry can be minuciously studied.

The RP of the cell 222 of the 1-D in the central fiber of the ischemic tissue turned out to be 211ms.

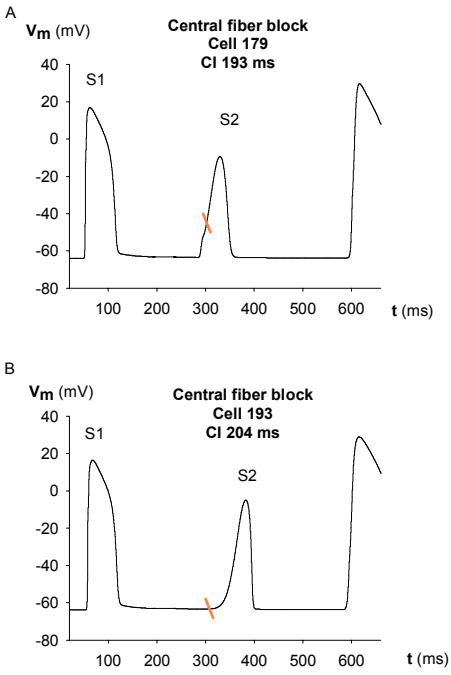


Figure 4. Membrane potential course and excitability recovery at block site in the central fiber at two different CIs. The end of refractoriness is highlighted by a oblique line. A: Example of a UDB due to refractoriness when CI of 193 ms (179 cell). B: Example of UDB in a completely recovered cell when CI of 204 ms (89 cell).

Figure 4 shows the time course of the membrane potential of the cell in the central fiber where propagation fails for two different CIs. Also, the end of refractoriness is represented by an oblique orange line. Panel A

describes the situation produced at CI 193 ms. In this case, the extraestimulus reaches this cell during its refractory period, so refractoriness is the direct cause of UDB generation. The opposite situation is depicted in panel B (CI=209 ms). In this panel, the cell is stimulated by S2 once its excitability has been recovered, so the final cause of the UDB does not lie on the refractoriness of the cell.

Our results show that refractoriness is the direct cause of UDB leading to reentry when the CI ranges from 170 to 193 ms. Hence, one third of the reentries are related to factors different from refractoriness, such as membrane excitability, involved in source-sink relationship mismatch that force UDB generation.

## 4. Discussion and conclusions

The analysis of the re-entries by means of SF during regional acute ischemia reveals that a) any extraestimulus whose CI ranged from 170 to 204 ms leads to reentry, b) the pattern of SF for reentrant electrical activity during regional ischemia has been characterized and c) UDB may not only be due to refractoriness but also to a mismatch in the source-sink ratio.

## Acknowledgements

This work h as been partially supported by the Plan Nacional de Investigación Científica, Desarrollo e Innovación Tecnológica del Ministerio de Educación y Ciencia of Spain (TEC2005-04199).

## References

[1] Wit AL, Janse MJ. The ventricular arrhythmias of ischemia and infarction: electrophysiological mechanisms. Futura Publishing Co. ed. Mount Kisko: 1993.

[2] Kuo C-S, Reddy CP, Munakata K, Surawicz B. Arrhythmias dependent predominantly on dispersion of repolarization. Cardiac Electrphysiology and Arrhythmias. 1985: 277-285.

[3] Coronel R. Heterogeneity in extracellular potassium concentration during early myocardial ischaemia and reperfusion: implications for arrhythmogenesis. Cardiovasc Res 1994; 28(6):770-777.

[4] Kleber AG, Rudy Y. Basic mechanisms of cardiac impulse propagation and associated arrhythmias. Physiol Rev 2004; 84(2):431-488.

[5] Qu Z, Karagueuzian HS, Garfinkel A, Weiss JN. Effects of Na(+) channel and cell coupling abnormalities on vulnerability to reentry: a simulation study. Am J Physiol Heart Circ Physiol 2004; 286(4):H1310-H1321.

[6] Shaw RM, Rudy Y. Ionic mechanisms of propagation in cardiac tissue. Roles of the sodium and L-type calcium currents during reduced excitability and decreased gap junction coupling. Circ Res 1997; 81(5):727-741.

[7] Wang Y, Rudy Y. Action potential propagation in inhomogeneous cardiac tissue: safety factor considerations and ionic mechanism. Am J Physiol Heart Circ Physiol 2000; 278(4):H1019-H1029.

[8] Effects of acute myocardial ischemia and its components on the safety factor of conduction: a simulation study. Lion, Francia: XXXII Computers in Cardiology Conference, 2005.

[9] Safety Factor in Simulated 2D Cardiac Tissue. Influence of Altered Membrane Excitability. Valencia, España: XXXIII Computers in Cardiology Conference, 2006.

[10] Faber GM, Rudy Y. Action potential and contractility changes in [Na(+)](i) overloaded cardiac myocytes: a simulation study. Biophys J 2000; 78(5):2392-2404.

[11] Ferrero JM, Jr., Saiz J, Ferrero JM, Thakor NV. Simulation of action potentials from metabolically impaired cardiac myocytes. Role of ATP-sensitive K+ current. Circ Res 1996; 79(2):208-221.

[12] Weiss JN, Venkatesh N, Lamp ST. ATP-sensitive K+ channels and cellular K+ loss in hypoxic and ischaemic mammalian ventricle. J Physiol 1992; 447:649-673.

[13] Yatani A, Brown AM, Akaike N. Effect of extracellular pH on sodium current in isolated, single rat ventricular cells. J Membr Biol 1984; 78(2):163-168.

[14] Irisawa H, Sato R. Intra- and extracellular actions of proton on the calcium current of isolated guinea pig ventricular cells. Circ Res 1986; 59(3):348-355.

[15] Coronel R, Fiolet JW, Wilms-Schopman FJ, Schaapherder AF, Johnson TA, Gettes LS et al. Distribution of extracellular potassium and its relation to electrophysiologic changes during acute myocardial ischemia in the isolated perfused porcine heart. Circulation 1988; 77(5):1125-1138.

[16] Walfridsson H, Odman S, Lund N. Myocardial oxygen pressure across the lateral border zone after acute coronary occlusion in the pig heart. Adv Exp Med Biol 1985; 191:203-210.

[17] Kagiyama Y, Hill JL, Gettes LS. Interaction of acidosis and increased extracellular potassium on action potential characteristics and conduction in guinea pig ventricular muscle. Circ Res 1982; 51(5):614-623.

[18] Watson CL, Gold MR. Effect of intracellular and extracellular acidosis on sodium current in ventricular myocytes. Am J Physiol 1995; 268(4 Pt 2):H1749-H1756.

[19] Sato R, Noma A, Kurachi Y, Irisawa H. Effects of intracellular acidification on membrane currents in ventricular cells of the guinea pig. Circ Res 1985; 57(4):553-561.

Address for correspondence

Lucía Romero Pérez
Universidad Politécnica de Valencia
Camino de Vera s/n
46071 Valencia
Spain
E-mail: lurope@doctor.upv.es